Multimode Interference-Based Two-Stage 1 × 2 Light Splitter for Compact Photonic Integrated Circuits

Milan L. Mašanović, *Student Member, IEEE*, Erik J. Skogen, *Student Member, IEEE*, Jonathon S. Barton, *Student Member, IEEE*, Joseph M. Sullivan, *Student Member, IEEE*, Daniel J. Blumenthal, *Fellow, IEEE*, and Larry A. Coldren, *Fellow, IEEE*

***Abstract*—A novel two-stage multimode interference 1 × 2 light splitter is proposed and fabricated in indium phosphide. The new splitter design is shorter by as much as 50% than a standard multimode-interference light splitter with the same output waveguide spacing. It has low inherent loss of 0.29 dB, low excess loss of 1.5 dB over 80-nm range, and imbalance of less than 0.25 dB over 100 nm.**

***Index Terms*—Beam splitting, multimode waveguides, optical beam splitting, optical planar waveguide components, waveguide components.**

I. Introduction

MULTIMODE interference (MMI)-based devices are important building blocks for photonic and optoelectronic integrated circuits due to their simple structure, low excess loss, large optical bandwidth, and low polarization dependence. These structures provide $N \times N$ power splitting–combining [1]–[3] for functions like 3-dB couplers, Mach–Zehnder interferometers (MZIs), ring lasers, and optical switches.

However, the typical length of standard design MMI splitter–combiners is longer than desired for functions that require the output waveguides be spaced far enough apart to minimize optical and electrical interaction (e.g., MZI wavelength converters). Minimizing the splitter–coupler length is desirable to realize more compact functional integrated optical circuits and for low propagation and scattering losses.

In this letter, the design for a novel two-stage 1 × 2 MMI light splitter is presented and experimental measurements described. The new splitter design demonstrates a large output waveguide separation (12 μm) with much shorter device lengths (500 μm) than comparable conventional designs (typical 1 mm) and exhibits even splitting ratios over 100-nm optical bandwidth. Another advantage of this design is in its compatibility with processes using wet crystallographic etches [7] that yield low-loss waveguides. Another class of light splitters that utilizes S-bends and/or Y-branches fabricated using reactive ion etching typically has higher scattering and/or radiation waveguide losses. While this other class of splitters can be compact (<500 μm), the total propagation losses (splitter + other waveguides) in a complex phontonic integrated circuit (PIC) will potentially be higher compared with wet etched waveguides.

Manuscript received October 4, 2002; revised January 2, 2003. This work was supported in part by DARPA under Grant MDA972-99-1-0006.

The authors are with the Electrical and Computer Engineering and Materials Departments, University of California, Santa Barbara, CA 93106 USA (e-mail: mashan@ece.ucsb.edu).

Digital Object Identifier 10.1109/LPT.2003.809972

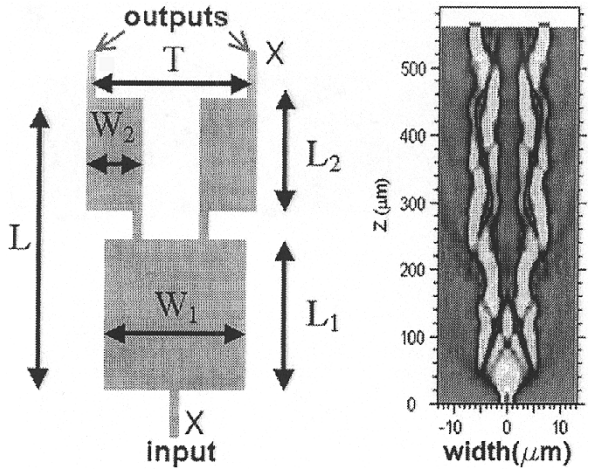

(a) (b)

Fig. 1. (a) Structure of the cascaded 1 × 2 splitter. (b) Beam-propagation method (BPM) simulation.

II. Device Structure and Design

MMI devices are based on the principle of self-imaging. An input field profile in a multimode waveguide is reproduced as single or multiple images at periodic intervals along the propagation direction of the waveguide, as a result of beating of different modes in the waveguide [1].

The beat length in a multimode waveguide is proportional to the square of the width of the multimode waveguide. In a standard 1 × 2 MMI light splitter, the width of the multimode region is equal to twice the desired output waveguide spacing. Therefore, in order to achieve the same output waveguide spacing T [Fig. 1(a)], we have designed a splitter that consists of two stages, and whose overall length is shorter than that of a standard MMI splitter. The new splitter layout is shown in Fig. 1(a).

The function of the first stage is to evenly split the incoming light. It is based on a standard 1 × 2 MMI splitter (MMI-1), using symmetric multimode interference as the light splitting effect [1]. The second stage is then used to increase the output waveguide spacing by offsetting the light from one edge at the input to the other edge at the output. This second stage consists of two identical 1 × 1 mirrored-image replicators (MMI-2) based on general multimode interference [1].

The separation of the output waveguides T, defined in Fig. 1(a), can be expressed as a function of the widths of MMI-1, MMI-2, and the input–output (access) waveguides X as

$$T = \frac{W_1}{2} + 2\,(W_2 - X) \tag{1}$$

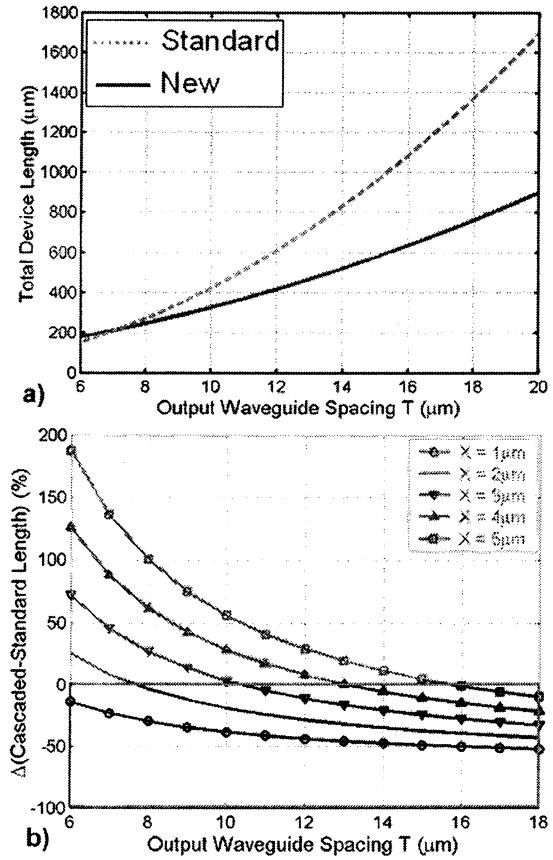

Fig. 2. (a) Length versus output waveguide spacing single and cascaded splitters. (b) Relative difference in length for cascaded and new splitter.

where W_1 and W_2 are effective widths of the MMI waveguides. Effective widths take into account the lateral penetration depth of each mode [1] and in our case they are close to actual physical dimensions of the MMIs. The total length of the splitter is equal to the sum of the components' lengths for MMI-1 and MMI-2, respectively,

$$L_{\text{total}} = \tfrac{3}{8}\,\rho W_1^2 + 3\rho W_2^2 \tag{2}$$

where ρ is constant for a given transverse waveguide geometry and wavelength [1]. Combining (1) and (2), for known output waveguide spacing T and access waveguide width X [Fig. 1(a)] results in a simple quadratic equation for total length, L_{total}, as a function of W_1 or W_2.

Finding the minimum of this function gives the following expressions for W_1 and W_2:

$$W_1 = \tfrac{2}{3}\,T + \tfrac{4}{3}\,X \tag{3}$$

$$W_2 = \frac{T}{3} + \frac{2}{3}\,X. \tag{4}$$

To illustrate the advantages of the proposed design, we performed calculations for InP-based devices with 1.4 Q quaternary waveguide [7]. Comparison of lengths of the standard and new 1 × 2 splitters as a function of the output waveguide spacing T is shown in Fig. 2(a). For $T = 12$ μm and $X = 2$ μm, the new splitter is 50% shorter.

Fig. 2(b) shows the relative difference in length between the standard and the new splitter as a function of output waveguide spacing, for various access waveguide widths X. The part of design space of interest is for $\Delta < 0$, where the new splitter is shorter. For most applications in the InP material system, the width of access waveguides will be 3 μm or less. For output waveguide separations large enough to achieve low optical, electrical, and thermal crosstalk, as well as to allow for reasonable processing tolerances ($T > 10$ μm), the new splitter design offers as much as 50% length reduction.

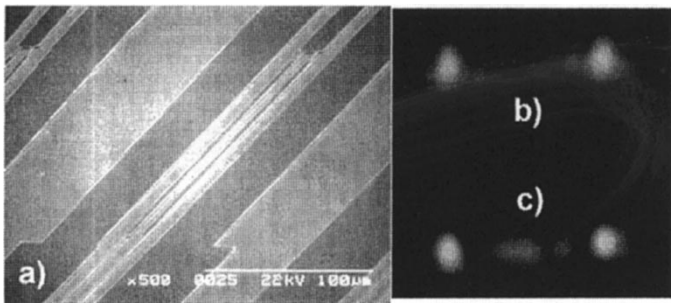

Fig. 3. (a) SEM image of the new splitter (detail). (b) Near-field image of the standard splitter. (c) Near-field image of the new splitter.

To verify the design of the new splitter, we have performed extensive simulations using the beam propagation method [Fig. 1(b)]. Device parameters for the simulations were adjusted and optimized according to our intended fabrication platform [7]. Optical loss inherent to this device was found to be 0.29 dB.

III. Fabrication and Experimental Results

We fabricated the new splitter using an offset quantum well InP PIC platform [7] [Fig. 3(a)]. Standard 1 × 2 splitters with identical output waveguide separation were fabricated on the same sample. For repeatable testing, both types of splitters were integrated with transverse electric polarized on-chip light emitting diodes (LEDs).

The epitaxial structure consisted of a 350-nm-thick quaternary InGaAsP 1.38Q waveguiding layer followed by a 10-nm-thick InP stop etch layer. A multiple (7) quantum-well region was grown on top of the stop etch layer, followed by a p-InP cap. The growth was performed using low-pressure metal–organic chemical vapor deposition. Quantum wells were selectively removed from the passive sections of the wafer and 1.8 μm of p-InP was regrown on top of it, followed by a 100-nm p+ InGaAs layer. After regrowth, ridges in InP were formed using wet chemical etching. Finally, top and bottom metal contacts (Ti–Pt–Au) were evaporated using E-beam evaporation. An scanning electron microscope (SEM) image of the new splitter is shown in Fig. 3(a). The length of the new splitter is 526 μm, whereas the length of the corresponding standard MMI splitter is 780 μm.

Near-field output images obtained for the standard 1 × 2 splitter and the new 1 × 2 splitter, in two separate measurements, are shown in Fig. 3(b) and (c), respectively. Both chip facets (LED and splitter side) were antireflection (AR) coated. Images were obtained using integrated LEDs biased at the same level as a light source and imaging the device output facet onto an infrared camera using a high numerical aperture lens. The

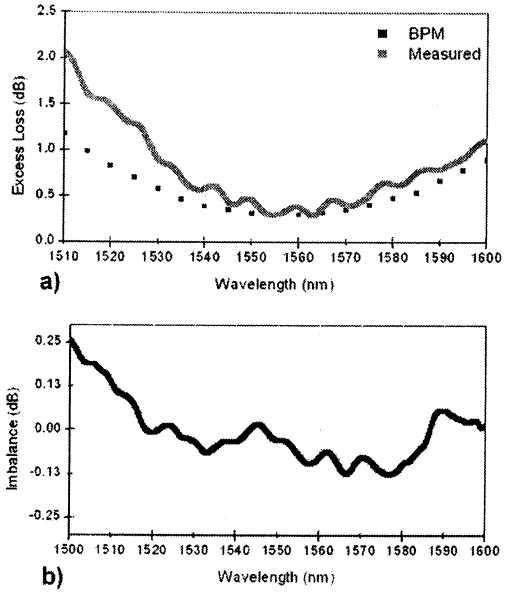

Fig. 4. (a) Splitter excess loss as a function of wavelength, and (b) splitter imbalance as a function of wavelength.

differences in the output spot sizes and shapes are attributed to the effect of spatial filtering of the output waveguides in the case of the new splitter. The light coming out of the new splitter propagates through additional 300 μm of quasi-single-mode waveguides before it reaches the facet—due to the difference in the length of the two splitters.

To fully characterize the new splitter, we have measured the excess loss and the power imbalance of the splitter as functions of wavelength. Again, we have used the LED on chip as a broad-band light source, and monitored the spectrum of the light coming out of both ends of the device (directly from the LED and from the splitter). The spectra were recorded using a high-resolution high-sensitivity optical spectrum analyzer.

We define excess loss as loss due to coupling, absorption, and index change with wavelength, given by

$$\alpha = -10 \cdot \log\left(\frac{P_{\mathrm{O1}} + P_{\mathrm{O2}}}{P_{\mathrm{O1\_opt}} + P_{\mathrm{O2\_opt}}}\right) + \alpha_{\mathrm{inh}} \qquad (5)$$

where P_{O1} and P_{O2} are output powers from output 1 and 2, respectively, $P_{\mathrm{01\_}opt}$ and $P_{\mathrm{02\_opt}}$ are output powers for the optimum wavelength, and α_{inh} is the inherent splitter loss. The result of our measurement is shown in Fig. 4(a). The excess loss is less than 1.5 dB over 80 nm. Fig. 4(a) also shows the comparison with simulated excess loss for our particular structure. The agreement between the two is good. Although our model for refractive index takes into account dispersion, we did not include changes of index due to change in absorption. That is the reason for walkoff of the two curves at lower wavelengths.

The power imbalance represents the ratio between measured output powers from the two splitter outputs as a function of wavelength and is given by

$$IB = 10 \cdot \log\left(\frac{P_{\mathrm{O1}}}{P_{\mathrm{O2}}}\right) \qquad (6)$$

where P_{O1} and P_{O2} have already been defined. The imbalance is measured to be less than 0.25 dB over 100 nm. We believe that the main cause for power imbalance is due to imperfect single-layer AR coating.

IV. Conclusion

A new, two-stage MMI-based light splitter is proposed and demonstrated. It can be as much as 50% shorter than a standard 1×2 MMI splitter with the same output waveguide spacing. Large output waveguide spacings are important for complex PIC applications such as integrated MZI structures. This splitter is suitable for fabrication using wet chemical etching, yielding PICs with low-loss waveguides. The splitter has low inherent loss, estimated to 0.29 dB, based on our BPM simulations.

The new splitter was fabricated in an InP–InGaAsP fabrication platform. The excess loss was measured to be 1.5 dB over 80 nm. Its output power imbalance was measured to be less than 0.25 dB over a 100-nm range. These characteristics make the two-stage splitter suitable for wavelength-division-multiplexing applications—realization of Mach–Zehnder and Michelson interferometers for low cost PICs [4], [5] (wavelength converters, modulators, heterodyne detectors).

References

[1] L. B. Soldano and E. C. M. Pennings, "Optical multi-mode interference devices based on self-imaging: Principles and applications," *J. Lightwave Technol.*, vol. 13, pp. 615–627, Apr. 1995.

[2] P. A. Besse, E. Gini, M. Bachmann, and H. Melchior, "New 2*2 and 1*3 multimode interference couplers with free selection of power splitting ratios," *J. Lightwave Technol.*, vol. 14, pp. 2286–2293, Oct. 1996.

[3] D. S. Levy, K. H. Park, R. Scarmozzino, R. M. Osgood, Jr., C. Dries, P. Studenkov, and S. Forrest, "Fabrication of ultracompact 3-dB 2*2 MMI power splitters," *IEEE Photon. Technol. Lett.*, vol. 11, pp. 1009–1011, Aug. 1999.

[4] B. Mikkelsen, T. Durhuus, C. Joergensen, R. J. S. Pedersen, S. L. Danielsen, K. E. Stubkjaer, M. Gustavsson, M. Van Berlo, and M. Janson, "10 Gbit/s wavelength converter realized by monolithic integration of semiconductor optical amplifiers and Michelson interferometer," in *Proc. ECOC'94*, vol. 4, Genova, Italy, 1994, pp. 67–70.

[5] D. A. Cohen, E. J. Skogen, H. Marchand, and L. A. Coldren, "Monolithic chemical sensor using heterodyned sampled grating DBR lasers," *Electron. Lett.*, vol. 37, pp. 1358–1360, 2001.

[6] P. A. Besse, M. Bachmann, H. Melchior, L. B. Soldano, and M. K. Smit, "Optical bandwidth and fabrication tolerances of multimode interference couplers," *J. Lightwave Technol.*, vol. 12, pp. 1004–1009, June 1994.

[7] X. Yan, M. L. Mašanović, E. J. Skogen, Z. Hu, D. J. Blumenthal, and L. A. Coldren, "Optical mode converter integration with InP–InGaAsP active and passive waveguides using a single regrowth process," *IEEE Photon. Technol. Lett.*, vol. 14, pp. 1249–1251, Sept. 2002.